Upcycling of Hemp Hurds into High-Value Cellulose Nanomaterials: Nanofibrillated Cellulose and Nanocrystalline Cellulose Production and Characterization

Ekrem Durmaz *

This study focused on the production and characterization of nanocellulose derived from hemp hurd, a highly valuable lignocellulosic natural resource. The holocellulose, alpha-cellulose, and lignin contents of the hemp hurd were determined as 83.3%, 39.1%, and 15.7%, respectively. The hemp hurd fiber had a length of 0.6 mm and a width of 19.1 µm. Following maceration and delignification pretreatments, bleached hemp hurd fibers were converted into nanofibrillated cellulose (NFC) by high-pressure homogenization, whereas nanocrystalline cellulose (NCC) was produced *via* sulfuric acid hydrolysis. The width of NFC was found to be 26.7 nm, while the width of NCC was determined to be 3.7 nm. The length of the NCC was confirmed to be 44.6 nm. The crystallinity indexes of NFC and NCC were found as 85.6% and 93.7%, respectively. The thermal decomposition of NFC occurred between 220 and 340 °C, whereas the thermal decomposition of NCC occurred between 170 and 550 °C. The residual material ratio was 25% for NFC and 28% for NCC. Moreover, the chemical bonds that form NFC and NCC, such as C–H, O–H, C–O–C, *etc.*, were identified.

DOI: 10.15376/biores.21.3.7893-7911

Keywords: Lignocellulosic natural resource; Hemp hurd; Nanofibrillated cellulose; Nanocrystalline cellulose

*Contact information: Kastamonu University, Faculty of Forestry, Department of Forest Industrial Engineering, 37150, Kastamonu, Türkiye; *Corresponding author: edurmaz@kastamonu.edu.tr*

INTRODUCTION

Hemp is a woody, annual plant from the Cannabaceae family. Originating in Asia, hemp has spread worldwide through various routes. Today, there are two subspecies: *Cannabis sativa* and *Cannabis indica*. The species important for industrial applications and used in fiber production is *Cannabis sativa*. The other species is banned worldwide due to its potential use as a drug. Hemp is one of the first cultivated plants in human history (Acar and Dönmez 2016). One readily available and reasonably priced natural fiber is industrial hemp (*Cannabis sativa*). Only a certain strain of *Cannabis sativa* may be grown in Europe and Canada, and it must contain no more than 0.2% tetrahydrocannabinol (THC) in Europe or 0.3% in Canada. Over the course of several centuries, hemp fiber has been produced for various applications, including ropes, sails, textiles, and papers (the first Bible copies were made from hemp paper). The hemp plant is indigenous to India and Persia, despite its cultivation in almost every temperate and tropical nation. With around one-third of the world's yearly production, Russia is the biggest producer of hemp fiber. Significant amounts of hemp fiber are also produced in other nations, including France, Germany,

Italy, Yugoslavia, Chile, China, Japan, and Peru. Hemp fiber has a lot of potential for use as reinforcement in composite materials because it is one of the strongest and most durable natural fibers available. An annual crop, hemp is tall and typically ready for harvesting two to three months after seeding. These fibers, which are found in the bast of the hemp plant, are similar in rigidity to glass fibers. The cross-sectional shape of hemp fiber is uneven and varies along its length. The major bast fibers, which are composed of roughly 70% to 74% cellulose, 15% to 20% hemicellulose, 3.5% to 5.7% lignin, 0.8% pectin, and 1.2% to 6.2% wax, span the whole length of the plant stem and are found in the phloem. There are also secondary bast fibers in the phloem that emerge from the cambium (Manaia *et al*. 2019). Figure 1 shows the hemp plant and its parts.

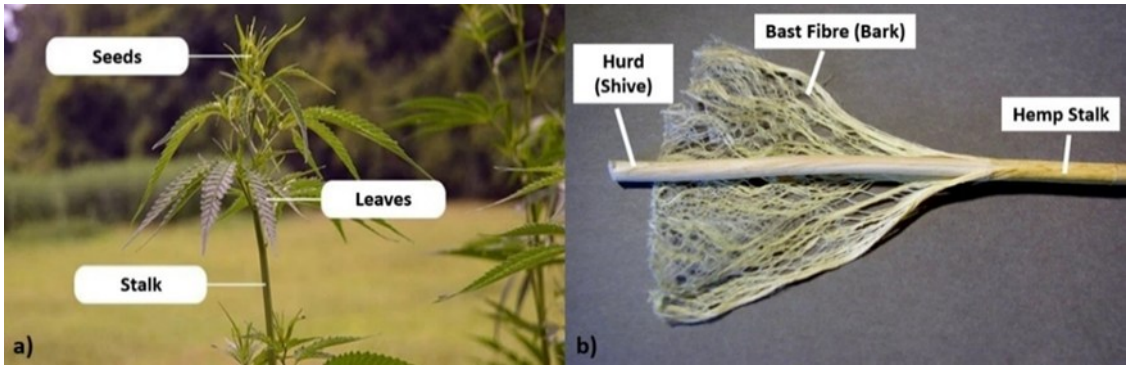

Fig. 1. a) Hemp (*Cannabis sativa*) plant (Reproduced from Vivek (2019)); and b) Parts of hemp plant (Reproduced from Lawson *et al.* (2022)). Both images are being used according to Creative Commons sharing terms.

The "bioeconomy" paradigm of this century encourages the use of renewable resources over nonrenewable ones in order to achieve both environmental sustainability and economic prosperity. Cellulose, the most prevalent polysaccharide in nature with an annual production of roughly 7.5×10^{10} tons, is being investigated as a versatile and renewable material because of the growing demand for ecological energy sources. Nanocellulose (NC), a special type of cellulose with dimensions less than 100 nm in at least one direction, has drawn interest from industry and researchers during the past few decades (Vu *et al*. 2024; Jankowska *et al*. 2025). High specific surface area, a good reinforcing capability, high strength, chemical resistance, high elastic modulus, biodegradability, biocompatibility, sustainability, lightweightness, high degree of polymerization, capacity to promote surface functionalization, thermal stability, high crystallinity, and environmental friendliness are among the special qualities of nanocellulose. Impregnated textiles, carbon dioxide adsorption, packaging, biomedical, construction, skin transplantation, texturing agent, cosmetics, paper and pulp, coatings and paints, electronics, sensing devices, composites, air filtration, water filters, *etc*., are just a few of the many potential applications for NC (Alvarado *et al*. 2024; Mo *et al*. 2024; Sukhikh *et al*. 2024; Al-Zu'bi and Fan 2025). Nanocellulose is predominantly found in three hierarchical structural forms: cellulose nanofiber (CNF) or nanofibrillated cellulose (NFC), which is pliable and elongated; cellulose nanocrystal (CNC) or nanocrystalline cellulose (NCC), which is rigid and short; and bacterial nanocellulose (BNC) or microbial cellulose, which is crystalline and pure. The highly crystalline NCC particles range in length from 100 nm to several μm and in width from 3 nm to 50 nm with 500 to 15000 polymerization degrees. With a length of up to 100 μm, a width of 5 nm to 100 nm and

higher than 500 polymerization degrees, NFC is a lengthy structure with both crystalline and amorphous regions. One of the primary forms of nanocellulose, BNC (4000 to 10000 polymerization degree, 4 to 50 nm width, and >500 nm length), is achieved from glucose molecules by the bacterial species *Gluconoacetobacter xylinus* through a bottom-up process. The characteristics of NC are influenced by the source of cellulose, extraction technique, application process, and degree of crystallinity or fibrousness (Padhi *et al*. 2023; Wang *et al*. 2024; Wossine *et al*. 2024). More detailed information on the production methods, properties, and application areas of NC types can be found in the studies conducted by Durmaz and Ates (2021, 2023a,b) and Durmaz *et al*. (2025). Furthermore, the literature contains a wealth of research and review articles, books, and book chapters on aforesaid these topics.

Over the past 20 years or more, growing environmental concerns have made a change in course necessary, particularly for companies that focus on chemicals. The development of "green chemistry", which promotes the production and use of bio-based products, is one of the most notable steps in this direction. Green chemistry is the general term for chemical processes that aim to reduce or eliminate the use of environmentally harmful substances, such as those based on petroleum and its derivatives. One of the primary goals is to maximize the efficiency of bio-based raw materials while minimizing waste emissions. Renewable bio-based products produced with the contribution of such raw materials are vital for eliminating the damage caused by environmental issues and creating a sustainable world. This study focuses specifically on the issues of renewability and sustainability. The hemp, used as a raw material for cellulose production, has been a biomass product produced in many places in Türkiye recently. Nanocellulose types derived from this annual herbaceous plant, along with the new generation of bio-based nanomaterials produced from them, will offer the opportunity to transform hemp beyond its traditional uses and convert this valuable plant into technological products. The primary objective of this study is to isolate nanofibrillated cellulose (NFC) *via* mechanical disintegration and nanocrystalline cellulose (NCC), through acid hydrolysis from hemp—an annually renewable and increasingly promoted crop in Türkiye—and to conduct their comprehensive physicochemical characterization, thereby elucidating the potential of this agricultural resource as a viable feedstock for nanocellulose production.

EXPERIMENTAL

Materials

In this study, hemp hurds, obtained by carefully separating the bast fibers from hemp (*Cannabis sativa*) stalks using a utility knife, were used as the raw material for the production of nanofibrillated cellulose (NFC) and nanocrystalline cellulose (NCC). The material was provided by the Hemp Research Institute of Ondokuz Mayıs University, Samsun, Türkiye. Nitric acid, sodium chlorite, sodium hydroxide, ethanol, acetic acid, chloroform, sulfuric acid, dialysis tubes, distilled water, and centrifuge tubes, as well as all laboratory glassware, consumables, machinery, and equipment, were supplied by the Forest Products Chemistry and Technology Laboratory in the Department of Forest Industrial Engineering, Kastamonu University, Türkiye. In addition, all chemicals used in production processes were procured from the several distributors of Sigma-Aldrich® and Thermo Fisher Scientific Inc. (Türkiye). The determination of chemical and morphological properties of hemp hurd and the production of NFC and NCC was performed in this

laboratory. On the other hand, the analyses for characterizations of NFC and NCC were performed at Kastamonu University Central Research Laboratory and Eskisehir Osmangazi University Center Research Laboratory Application and Research Center as well as the Polymer Research Laboratory.

Methods

Determination of chemical components of hemp hurd

Samples prepared for chemical analysis should be representative of the population, *i.e.*, the entire material from which the sample was obtained. The following analyses were conducted in accordance with TAPPI standards for the chemical characterization of hemp hurd fiber. All experiments were performed in triplicate, and the average values were calculated. Prior to the analyses, the moisture content of the hemp hurd samples was determined to be 5.7%.

- Preparation of wood for chemical analysis (TAPPI T 264 om-07, 2007)
- Solvent extractives of wood and pulp (TAPPI T 204 cm-97, 1997)
- Acid-insoluble lignin in wood and pulp (TAPPI T 222 om-02, 2002)
- Holocellulose content of wood and pulp (Wise's Chlorite method (1946))
- Alpha-, beta- and gamma-cellulose in pulp (TAPPI T 203 cm-99, 1999)
- One percent sodium hydroxide solubility of wood and pulp (TAPPI T 212 om-12, 2012)
- Water solubility of wood and pulp (TAPPI T 207 cm-99, 1999)
- Ash in wood, pulp, paper and paperboard: Combustion at 525ºC (TAPPI T 211 om-02, 2002)

Determination of morphological properties of hemp hurd

To determine the morphological properties of hemp hurd fiber, nitric acid maceration, as applied by Mahesh *et al*. (2015), was used to release the fibers. The softened samples were separated into their fibers using a mechanical stirrer at 500 rpm. Fibers with magnifications with the 4× and 10× objective lenses were used to determine fiber length, and objectives with magnifications of 20× and 40× were used to determine fiber width, lumen width, and fiber wall thickness. Morphological measurements were performed on fiber images obtained with a SOIF (BK5000-TR/L, CHINA) microscope using the Digimizer Image Analysis Software 6.5.0 program. The obtained morphological characteristics (fiber length, fiber width, lumen width, and fiber wall thickness) were used to determine fiber-size relationships (felting ratio, elasticity coefficient, rigidity coefficient, Muhlstep ratio, Runkel ratio, and F factor), which are of great importance in papermaking. For this purpose, the following formulas were used (Tank *et al*. 1990):

- Felting ratio: Fiber length / Fiber width
- Elasticity coefficient: Lumen width × 100 / Fiber width
- Rigidity coefficient: Fiber wall thickness × 100 / Fiber width
- Muhlstep ratio: Fiber wall area × 100 / Fiber cross-sectional area
- Runkel ratio: 2 × Fiber wall thickness / Lumen width
- F factor: Fiber length x 100 / Fiber wall thickness

Pre-treatments for NFC and NCC production

Before the production of NFC and NCC, hemp hurds were cut into lengths of 2 to 3 cm. They were then subjected to two processes: first, nitric acid maceration, followed by delignification/bleaching steps using sodium chloride ($NaClO_2$) and acetic acid (CH_3COOH) (Xu *et al*. 2018; Nagarajan *et al*. 2021; Amara *et al*. 2025). In nitric acid maceration, the method applied by Mahesh *et al*. (2015) was conducted. According to this method, the raw materials were boiled in a 50% nitric acid solution at 80 °C for 6 h and finally washed with approximately 5 L of distilled water until the acid content was removed. The delignification process was applied to hemp hurd samples that were fibrous by maceration. In this process, Wise's chlorite method (Wise *et al*. 1946) was used. Macerated hemp fibers were treated in a sodium chlorite/acetic acid solution at 80 °C. Sodium chlorite/acetic acid was added to the solution at one-hour intervals, and this process was repeated 5 times. At the end of the process, the fibers were thoroughly washed with distilled water. The macerated and delignified hemp hurd samples were dried in the oven and made ready for NFC and NCC production.

Production of NFC

In NFC production, the method applied by Espinosa *et al*. (2022) and Ang *et al*. (2019) was implemented with some modifications. NFC production is briefly described as follows: The macerated and bleached hemp hurd fibers were kept in the oven until they were completely dry. A suspension was prepared in a 1.0 L volume at a 1% concentration from fibers with full dry weight. The suspension was mixed using a high-speed blender with a 1.8-L container capacity (Karaca Inox Powermix Smoothie Blender 1801, 1800 W) at 10,000 rpm for 10 min to ensure homogeneous distribution of the fibers. This process was repeated 4 times. The resulting suspension was treated in a high-speed homogenizer, brand Velp Scientifica OV5 Homogenizer, at 15000 rpm for 10 min, and this process was repeated four times. In the next step, the homogeneous suspension was transferred to the GEA Panda-Plus 2000 brand high-pressure homogenizer for NFC production. The suspension was treated 10 times under a pressure of approximately 1000 bar (15000 PSI). To prevent any bacterial or fungal growth, a few drops of chloroform were added to the NFC suspension, and it was stored at +4°C.

Production of NCC

In NCC production, the acid hydrolysis process applied by Beltramino *et al*. (2016) as well as Lu and Hsieh (2012) were used with minor modifications, and sulfuric acid was preferred for this method. In summary, cellulosic pulps were treated in a 64% sulfuric acid solution. Here, the pulp/acid ratio was set at 1:10 (g/mL). Acid hydrolysis was performed in a fume hood at 50 °C for 1.0 h. After acid hydrolysis, the reaction was stopped by adding five times the sample/acid volume of distilled water to the system. The suspension was then transferred to a centrifuge and processed at 5000 rpm for 10 min. The centrifugation process was repeated 5 times. After each repetition, the supernatant in the tubes was replaced with distilled water. Following centrifugation, the supernatant and precipitate in the tubes were mixed for 15 min using a mechanical stirrer to obtain a homogeneous suspension. The homogenized NCC suspension was transferred to dialysis tubes with a molecular weight of 12,000 to 14,000 Daltons for dialysis treatment, and these tubes were immersed in distilled water and left to stand until their pH reached 7 (approximately a week). The pure water used was replaced daily. To remove acid residues from the NCC suspension after dialysis, a second centrifugation process was performed using the same

parameters as the first process. Finally, to separate the clustered NCC particles, the suspension was subjected to ultrasonication in an ultrasonic bath at 53 kHz for 15 min.

Characterization of NFC and NCC

Dynamic light scattering (DLS) analysis

Dynamic light scattering (DLS) analysis was performed for the morphological evaluation of NFC and NCC samples. Although this analysis is generally applied to nanoparticles with spherical morphology, it also provides information on the particle size distributions of NFC and NCC. Suspensions with a concentration of 0.1% were used for DLS analysis with Zetasizer Nano ZS instrument (Malvern, UK). The measurements were conducted at Eskişehir Osmangazi University Polymer Research Laboratory.

Zeta potential analysis

Zeta potential values of NFC and NCC were determined with a zeta potential measurement device (Zetasizer Nano ZS instrument; Malvern, UK) at 0.1% concentration. The measurements were carried out at Eskişehir Osmangazi University Polymer Research Laboratory.

Scanning electron microscopic analysis

For morphological examination of the raw material, bleached fiber, NFC and NCC samples, a Quanta FEG 250 (USA) scanning electron microscope (SEM), located in Kastamonu University Central Research Laboratory was used. Before imaging, NFC suspensions were diluted to a concentration of 0.01% and dried with a vacuum dryer. The samples were coated with gold for 2 min using a sputter coater (Sputter Coater 108 Auto; Cressington, Watford, UK) before imaging.

Transmission electron microscopic analysis

A JEOL 1220 JEM (JEOL Ltd., Tokyo, Japan) transmission electron microscope (TEM) located in the Application and Research Center of Eskişehir Osmangazi University Central Research Laboratory was used for imaging NFC and NCC samples. Because TEM analysis provides information about the delicate structures of tiny samples, raw material and bleached fiber samples were not included in this analysis. Before analysis, the concentrations of NFC suspensions were diluted to 0.05%, while those of NCC were 0.005%, and these suspensions were placed on formvar films supported by copper TEM grids, using a micropipette. The prepared grids were used for imaging.

X-ray diffraction analysis

The crystallinity properties of the samples were determined with a Bruker D8 Advance (Billerica, MA, USA) brand X-ray diffraction device at the Kastamonu University Central Research Laboratory. This analysis was carried out using CuKα radiation at a wavelength of λ = 0.15418 nm, with a 2θ value in the range of 5° to 80°. Additionally, diffraction data were obtained at 2θ = 0.05° step spacing and 3 s/step time.

Fourier transform infrared spectroscopic analysis

The chemical bond structures of the samples were determined using the Bruker Alpha FTIR device (Billerica, MA, USA) at the Kastamonu University Central Research Laboratory. Each sample was analyzed at a scanning resolution of 4 cm^{-1} and a band range of 4000 to 650 cm^{-1}.

Thermogravimetric analysis

The samples' thermal characteristics were ascertained using the TGA apparatus (TGA-DTA Hitachi STA7300; Tokyo, Japan), located in the Kastamonu University Central Research Laboratory. Tests were carried out between 25 and 800 °C in a nitrogen gas atmosphere, with a temperature increase of 10 °C/min.

Differential scanning calorimetry analysis

In addition to TGA analysis, DSC analysis was also used to determine the thermal properties of the samples. These tests were done using a Hitachi DSC7020 (Tokyo, Japan) DSC apparatus, located at the Kastamonu University Central Research Laboratory. Nitrogen gas was used with a temperature increase of 10 °C/min between 25 °C and 400°C.

RESULTS AND DISCUSSION

Chemical Components of Hemp Hurd

The holocellulose content of hemp hurd was found to be 83.3%; alpha cellulose content 39.1%; lignin content 15.7%; and ash content 1.8%. Furthermore, the solubility in alcohol, 1% NaOH, hot water, and cold water was determined to be 4.8%, 31.7%, 9.9%, and 5.9%, respectively. In his study with hemp bast, Gümüşkaya (2002) determined the ratios of holocellulose, cellulose, α-cellulose, and lignin as 86.9%, 71.4%, 63.8%, and 6.6%, respectively. Manaia *et al*. (2019) found that hemp stalk (husk) fibers have a cellulose content of 70% to 74%, a lignin content of 3.5% to 5.7%, a hemicellulose content of 15% to 20%, a pectin content of 0.8%, and an ash content of 0.8%. In another study, Tyagi *et al*. (2021) utilized nanofibers obtained from hemp tow, applying various processes to produce films with advanced barrier properties. They determined the lignin content of the hemp to be between 23% and 24% and the extractive substance content between 2% and 5%. A study by Barybina *et al*. (2024) produced microcrystalline cellulose from hemp tow and investigated some of its properties. The percentages of cellulose, hemicellulose, lignin, and inorganic components in the hemp tow used as raw material were determined to be 48.4%, 25.8%, 20.9%, and 2.7%, respectively.

Morphological Properties of Hemp Hurd

Microscopic images of the separated individual hemp hurd fibers are given in Fig. 2. Microscopic measurements revealed that the hemp hurd fiber had a fiber length of 0.6 mm, a fiber width of 19.1 µm, a lumen width of 11.3 µm, and a fiber wall thickness of 3.8 µm. Morphological studies conducted on different parts of the hemp plant can be found in the literature. In their review of flax and hemp, Manian *et al*. (2021) stated that the hemp fiber length ranged from 0.5 to 0.6 mm and its width from 15 to 40 µm. Li *et al*. (2013), in their research examining the morphological characteristics of hemp stalk fibers taken from different stem heights, determined the lengths of the samples to be between 0.51 and 0.57 mm, their diameters between 25.6 and 32.2 µm, their lumen diameters between 6.25 and 11.9 µm, and their cell wall thicknesses between 4.34 and 5.92 µm. In another study, Ateş *et al.* (2011) investigated the morphological characteristics of hemp bast fibers. The fiber length, fiber width, lumen width, and fiber wall thickness of the samples were found to be 28.74 mm, 25.53 µm, 7.54 µm, and 8.99 µm, respectively.

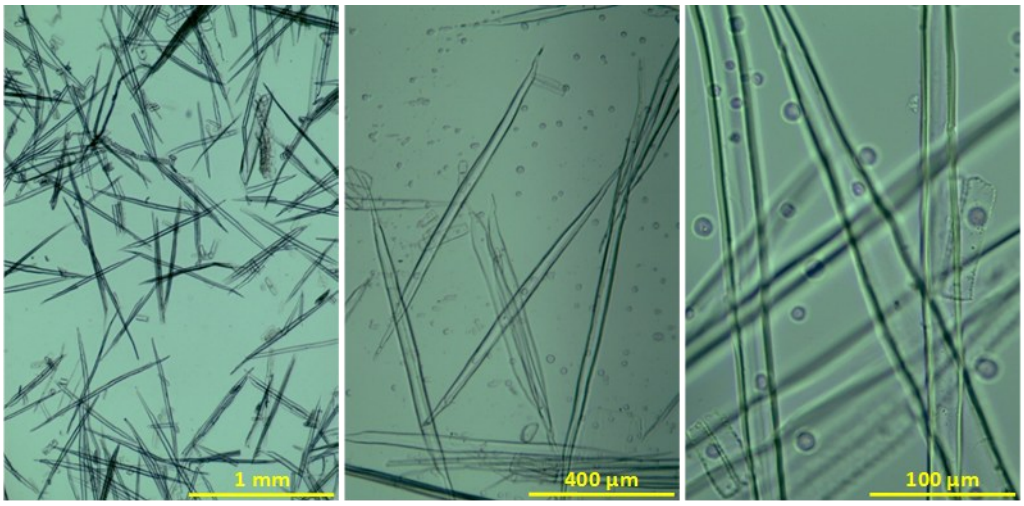

Fig. 2. Microscopic images of hemp hurd fibers

The felting ratio of hemp hurd fibers was determined as 32.9; the elasticity coefficient as 59.4; the rigidity coefficient as 20.2; the Muhlstep ratio as 64.6; the Runkel ratio as 0.6; and the F factor as 16237. These values are important for paper production. These results suggest that hemp hurd fibers may serve as a promising alternative raw material for pulp and paper production.

Zeta Potentials and Size Distributions of NFC and NCC

As a result of DLS analyses, the equivalent spherical diameters of NFC and NCC obtained from hemp were determined to be 4041 nm and 778 nm, respectively. Figure 3 shows the DLS graphs of NFC and NCC samples in terms of intensity, number, and volume. The pH of the suspensions subjected to zeta potential analysis was determined to be 6.5 for NFC and 6.2 for NCC. The zeta potentials and electrical conductivities of these samples were determined as -36.8 mV and 0.38 mS/cm for NFC as well as -39.8 mV and 0.64 mS/cm for NCC, respectively. The zeta potential of the NCC sample was higher than that of the NFC sample. When examining the literature on hemp in terms of zeta potential analysis, similar values were found. In their study, Heacock *et al*. (2024) investigated the properties of cellulose nanocrystals (CNC) obtained from industrial hemp waste and determined the zeta potential value of these samples as -38.6 mV. In another study, Beluns *et al*. (2021) confirmed the zeta potential of nanofibrillated cellulose (NFC) produced from hemp stalks to be -22.6 mV.

Morphological Properties

The SEM and TEM images of raw material, bleached fiber, NFC, and NCC are given in Fig. 4. The SEM image in Fig. 4A shows hemp as a raw material. The bleached fiber SEM image in Fig. 4B shows that lignin has been removed from the raw hemp material after maceration and delignification processes, and the fibers have been separated. The SEM image in Fig. 4C and the TEM image in Fig. 4E show NFC, which has an entangled structure and contains both crystalline and amorphous regions of cellulose.

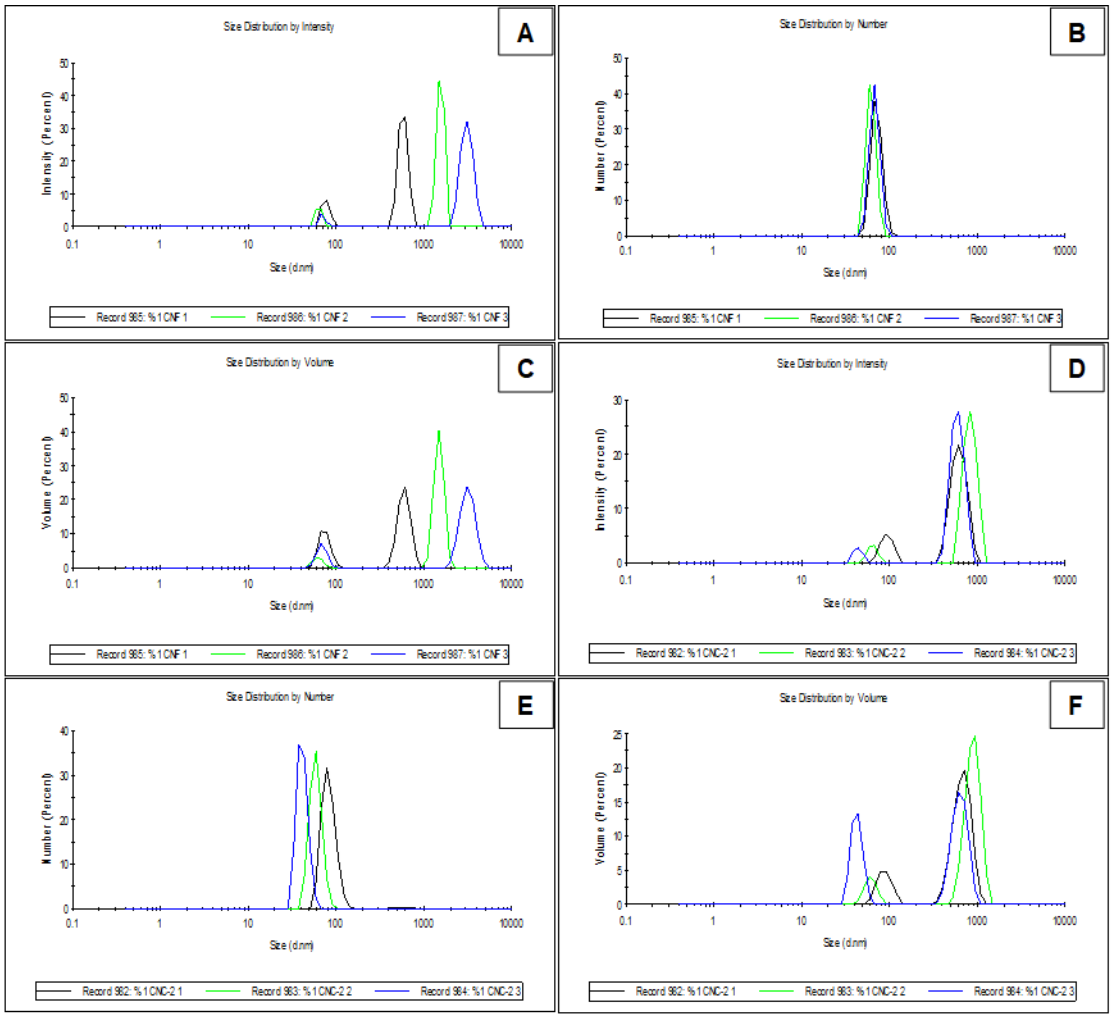

Fig. 3. DLS analysis results of NFC in terms of A) Density; B) Number; C) Volume; and NCC in terms of D) Density; E) Number; F) Volume

Examination of the SEM images in Fig. 4D and the TEM images in Fig. 4F reveal that NCC has a needle-like structure. It contains only the crystalline region of cellulose. Figures 4C and 4E demonstrate the successful application of mechanical disintegration on bleached hemp fibers, while Figs. 4D and 4F prove that sulfuric acid hydrolysis removes amorphous regions from bleached hemp cellulose with high efficiency. The widths of the samples were determined as 331 µm for raw material, 5.4 µm for bleached fiber, and 26.7 nm for NFC. The width of NCC was determined as 3.7 nm, and its length as 44.6 nm.

These results confirm the effectiveness of the applied chemical and mechanical treatments in producing nanocellulose with substantially reduced dimensions and well-defined nanoscale morphology. Norfarhana *et al*. (2025) produced NFC from sugar palm fibers using a wet disk milling method following ionic liquid pretreatment. They determined the diameter of the NFC to be approximately 3.30 ± 0.68 nm. Tiwari and Sanjog (2025) found that the CNC extracted from Indian water chestnut shells had a length of 265 nm and a width of 83 nm. In another study, Ratnakumar *et al*. (2021) observed that the diameters of NFC produced from rice husk ranged between 100 and 200 nm. Xu *et al*. (2018) found that the diameter of the CNF they produced from waste corn stover ranged from 5 to 50 nm, and its length was a few micrometers.

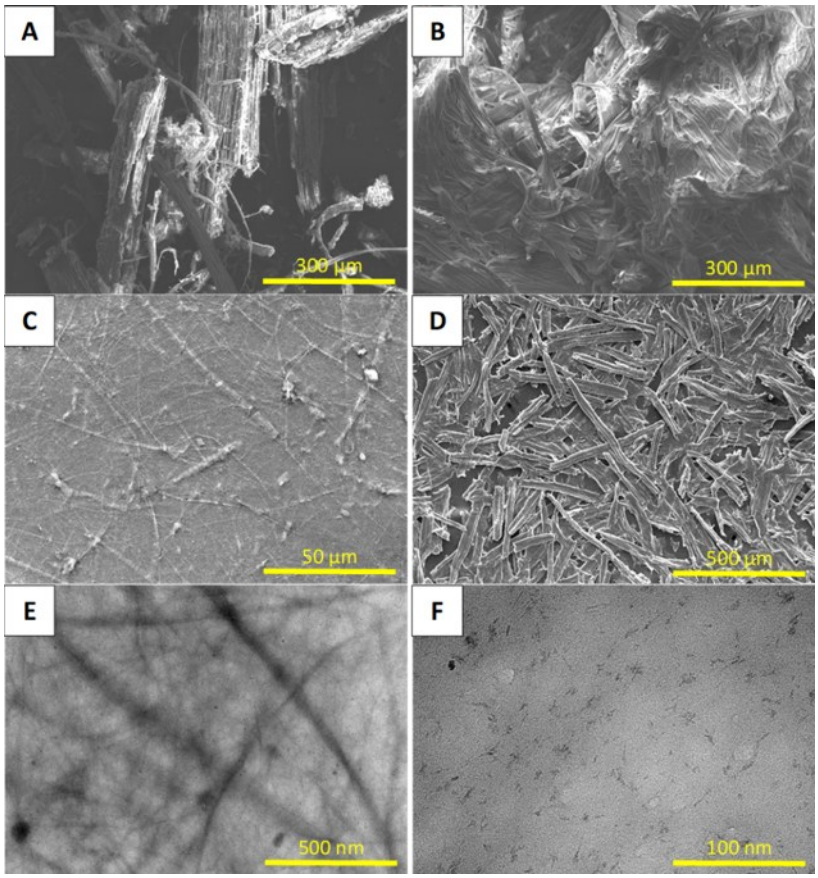

Fig. 4. Images of hemp hurd samples A) SEM image of raw material; B) SEM image of bleached fiber; C) SEM image of NFC; D) SEM image of NCC; E) TEM image of NFC; and F) TEM image of NCC

Crystallinity

The crystallinity index (CI) determines the orientation of cellulose crystals in a fiber concerning the fiber axis. The CI is detected by the values given by the 2θ angle near 22º and 18º in X-ray diffraction (XRD) analysis. The crystalline portions of the cellulosic material are represented by 22º, while the amorphous portions are represented by 18º. Consequently, the following formula is used to determine the samples' crystallinity index (Reddy and Yang 2005):

$$\text{CI (\%)} = \frac{I_{22} - I_{18}}{I_{22}} \text{ x } 100 \quad (1)$$

In Eq. 1, I_{22} and I_{18} symbolize the intensity values at the 2θ angles obtained near 22° and 18°, respectively.

The crystallinity results of hemp as raw material, bleached fiber, NFC, and NCC are given in Fig. 5. The peak at 22° on the 2θ-scale axis of the graphs demonstrates the crystalline regions of the samples, whereas the peak at 18° reflects the amorphous regions of the samples. The crystallinity indexes of raw material, bleached fiber, NFC, and NCC were determined as 66.8%, 84.5%, 85.6%, and 93.7%, respectively. It was observed that the crystallinity index (CrI) of the raw hemp material was increased as a result of the bleaching process. It was also determined that the crystallinity index of NCC was greater than that of NFC. This situation is explained by the acid hydrolysis process, which removes the amorphous regions of cellulose and releases the crystalline regions. Similar studies can

be found in the literature. Jiang and Gu (2020) investigated the crystallinity properties of nanocrystalline celluloses (NCCs) produced from different renewable sources (softwood pulp, microcrystalline cellulose, bagasse and cotton straw). The crystallinity indexes of the NCCs were determined to be 72.1% for softwood pulp, 76.2% for microcrystalline cellulose, 68.6% for bagasse, and 70.8% for cotton straw. Stanislas *et al*. (2022) produced nanofibrillated cellulose (NFC) from raffia fiber and cassava bagasse. According to the XRD analysis results, the crystallinity indexes of the samples were determined as 45%, 51%, and 62% for raffia fiber, pulp, and NFC, respectively, while they were found to be 9%, 38%, and 57% for cassava bagasse fiber, pulp, and NFC, respectively. Kian *et al*. (2018) determined the crystallinity index of NCCs produced from roselle-derived microcrystalline cellulose to be 76.2%, 77.7%, and 79.5% for samples subjected to acid hydrolysis for 30, 45, and 60 minutes, respectively. Lee *et al.* (2017) produced nanocrystalline cellulose (NCC) from eucalyptus wood and rice straw *via* sulfuric acid hydrolysis conducted for 30, 45, 60, 75, 90, and 120 min. The highest crystallinity indices were observed after 45 min of hydrolysis, reaching 76.1% for the wood-derived sample and 76.3% for the rice straw–derived sample.

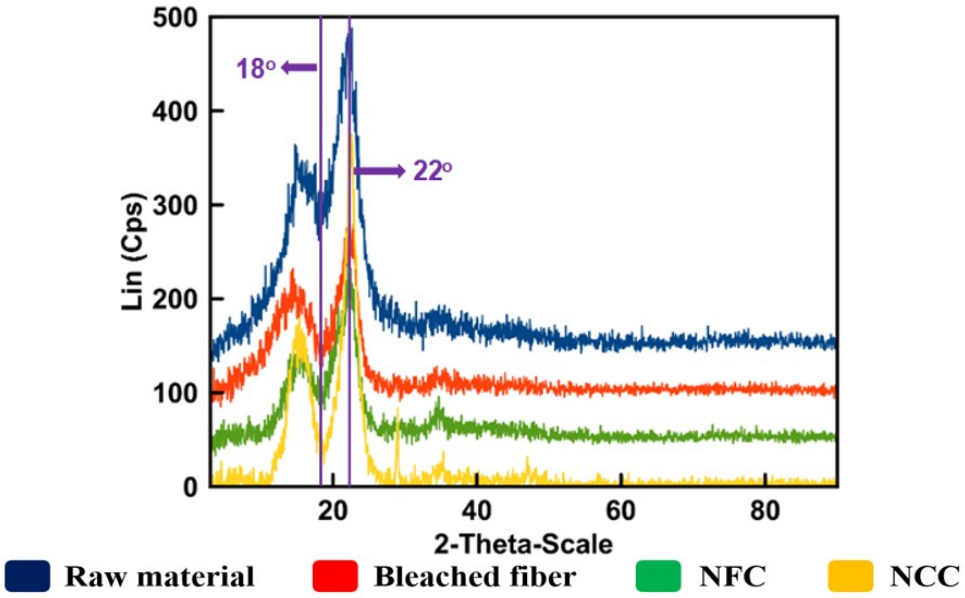

Fig. 5. XRD results of hemp hurd samples

Thermal Properties

The thermal properties of all samples are demonstrated in TGA and DSC graphs in Figs. 6A and 6B, respectively. The mass loss up to 100 °C in the TGA graph for all samples is owing to the removal of moisture in the samples. According to Fig. 6A, it was confirmed that the main thermal decompositions for hemp happened approximately between 250 and 370 °C in raw material; between 240 and 350 °C in bleached fiber; between 220 and 340 °C in NFC; and between 170 and 550 °C in NCC. After thermal decomposition, it was determined that 16% of residual materials was released from the raw material and bleached fiber, 25% from NFC, and 28% from NCC. When the TGA graph is examined, the degradation onset temperatures of the raw material and bleached fibers are found to be higher compared to those of the NFC and NCC samples. In contrast, the residual amounts of the raw material and bleached fibers are lower than those of the NFC and NCC samples.

NCC began to decompose at lower temperatures compared to the other samples. The reason for this is thought to be that NCC does not contain amorphous regions of cellulose but consists only of crystalline regions, and that the sulfate groups on NCC surface also cause this situation. The NFC exhibited better thermal resistance than NCC, but its thermal degradation occurred at lower temperatures compared to the raw material and bleached fiber samples. Although more residual material was released in the NCC sample after thermal decomposition, this sample type started to decompose at much lower temperatures compared to the others, and the decomposition process took longer. The crystalline and amorphous regions contained in the raw material, bleached fiber, and NFC samples ensured that these samples exhibited better thermal properties than the NCC sample consisting of only crystalline regions.

The DSC graph in Fig. 6B provides information about the glass transition temperatures of the samples. The endothermic curves detected between 50 and 150 °C in the DSC graph of raw material, bleached fiber, and NFC were formed owing to the evaporation of moisture in the samples. The main thermal decomposition of all samples happened above 250 °C. In NCC sample, the first endothermic peak emerged above the decomposition temperature of the sample, which was 200 °C. This situation demonstrates that the thermal degradation of NCC occurs at lower temperatures. Ganesan and Rengarajan (2024) successfully isolated NFC from sugarcane bagasse and pineapple leaves and systematically evaluated its thermal behavior. Thermogravimetric analysis revealed that degradation events occurring at approximately 210 °C and 400 °C were attributable to the decomposition of hemicellulose/lignin fractions and α-cellulose, respectively. In chemically treated fiber samples, the mass loss observed within the temperature range of 340 to 413 °C was associated with cellulose degradation. Moreover, the principal degradation stage identified between 310 and 403 °C was assigned to the thermal decomposition of NFC, indicating its characteristic thermal stability profile. Jasmani *et al*. (2022), in a study examining NFC and NCC produced from *Macaranga gigantea* wood, reported that the thermal decomposition of the raw material, unbleached pulp, bleached pulp, NFC, and NCC samples occurred over a temperature interval of 200 to 490 °C. The primary thermal degradation stage was determined to begin at approximately 200 °C and extend to nearly 380 °C, corresponding to the decomposition of hemicellulose and cellulose constituents. For all samples except NCC, the onset of cellulose degradation occurred at around 270 °C. In contrast, NCC exhibited an earlier initiation of cellulose decomposition at approximately 200 °C, followed by a secondary degradation phase between 310 °C and 490 °C. The comparatively lower thermal stability of NCC relative to the other samples was attributed to the presence of sulfate ester groups on its surface. In another study, Zhang *et al*. (2020) isolated NFC from *Enteromorpha prolifera* and prepared NCC from commercially available microcrystalline cellulose (MCC). Thermogravimetric analysis revealed that the onset decomposition temperature (T_{onset}) and the maximum degradation temperature ($T_{d,max}$) of NFC were 280 °C and 322 °C, respectively. In contrast, NCC exhibited significantly lower thermal stability, with the corresponding T_{onset} and $T_{d,max}$ values of 187 °C and 245 °C. Again, the reduced thermal stability of NCC was attributed to the incorporation of sulfate ester groups during sulfuric acid hydrolysis, which are known to promote earlier thermal degradation.

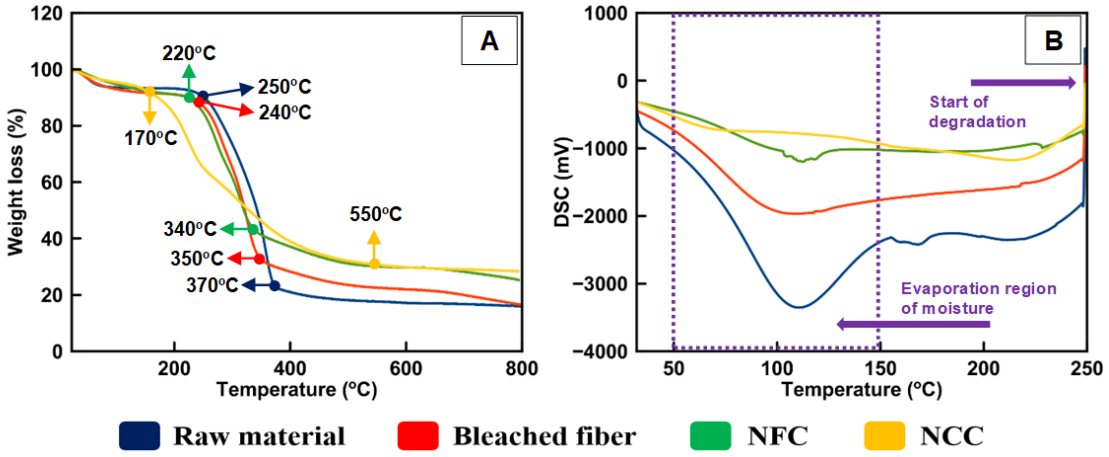

Fig. 6. A) TGA and B) DSC results of hemp hurd samples

Chemical Bond Structures

The chemical bond structures of hemp hurd samples as raw material, bleached fiber, NFC, and NCC are presented in the FTIR graphs in Fig. 7. The strong peaks observed between 3400 and 3100 cm^{-1} wavelengths in all samples indicate the presence of −OH bonds in carbohydrates (Singh *et al*. 2020). These peaks appeared at frequencies of 3325 cm^{-1} for raw material, 3331 cm^{-1} for bleached fiber, 3342 cm^{-1} for NFC, and 3339 cm^{-1} for NCC. Similarly, the vibration detected at a frequency of 2981 cm^{-1} in all samples reflects the C–H bond, indicating the presence of organic molecules in the samples. The peak observed at 1748 cm^{-1} in the raw material sample is attributed to the stretching vibration of the acetyl and uronic ester groups in the ester bond of the carboxyl group of pectin, hemicellulose, or lignin and/or the ferulic and *p*-coumaric acids of hemicelluloses. This vibration was not observed in bleached fiber, NFC, and NCC samples. The absence of this vibration in these samples proves that the bonds forming lignin and hemicelluloses are removed by bleaching, mechanical, and acid hydrolysis processes (Akinjokun *et al*. 2021). The bands identified at frequencies of 1158 cm^{-1} and 1053 cm^{-1} in the raw material sample reflect the asymmetric stretching of the C–O–C glycosidic bond and the C–O–C vibration in the pyranose ring, respectively (Zhong *et al*. 2024). Similarly, strong vibrations identified in the raw material, bleached fiber, NFC, and NCC samples at bands of 1027 cm^{-1}, 1021 cm^{-1}, 1028 cm^{-1}, and 1026 cm^{-1}, respectively, also indicate C–O–C stretching in the pyranose ring (Krishnadev *et al*. 2020). The vibration observed at 899 cm^{-1} belongs to the α-glycosidic bonds of the glucose ring in the cellulose content (Singh *et al*. 2020). The peaks determined in the 1428 cm^{-1} band in NFC and in the 1422 cm^{-1} band in NCC show symmetrical bending of the CH_2 bond and indicate the high crystallinity of nanocelluloses (Jamaluddin *et al*. 2024). The peak at 1628 cm^{-1} in the NCC sample can be attributed to the C–O stretching of the acetyl group in cellulose. Furthermore, between frequencies of 1385 cm^{-1} and 1365 cm^{-1}, C–H bending vibrations and C–O stretching vibrations occur for saturated aliphatic species. These vibrations peaked at 1367 cm^{-1} in raw material, 1366 cm^{-1} in bleached fiber, 1366 cm^{-1} in NFC, and 1371 cm^{-1} in NCC. These detected peaks reveal the C–H bending of the alkyl group and the C–O stretching of the hydroxyl group in cellulose (Tiwari and Sanjog 2025).

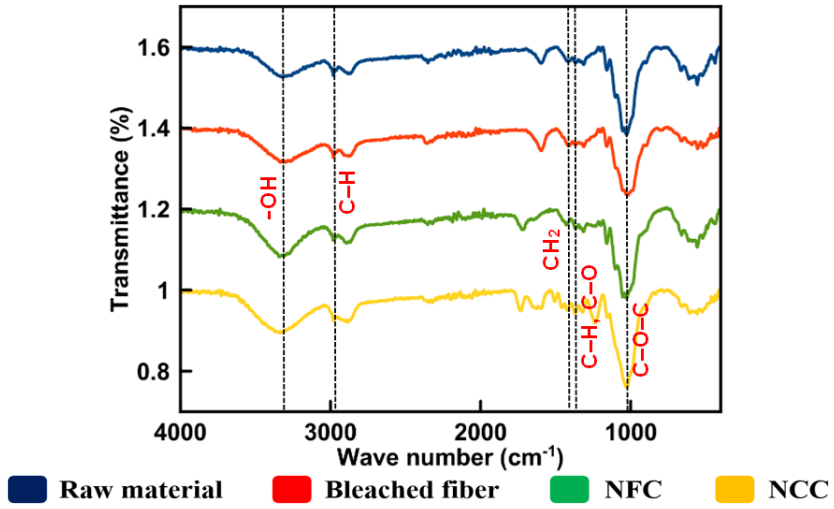

Fig. 7. FTIR results of hemp hurd samples

CONCLUSIONS

1. Holocellulose, alpha cellulose, lignin, and ash contents of hemp hurd were determined as 83.3%, 39.1%, 15.7%, and 1.8%, respectively, while alcohol, 1% NaOH, hot water, and cold water solubilities of hemp hurd were confirmed as 4.8%, 31.7%, 9.9%, and 5.9%, respectively. Hemp hurd fiber averaged 0.6 mm in length, 19.1 µm in width, 11.3 µm in lumen width, and 3.8 µm in fiber wall thickness. In addition, the felting ratio of hemp hurd fibers was established as 32.9; the elasticity coefficient as 59.4; the rigidity coefficient as 20.2; the Muhlstep ratio as 64.6; the Runkel ratio as 0.6; and the F factor as 16237.
2. The equivalent spherical diameter and zeta potential of NFC were 4041 nm and -36.8 mV, whereas the equivalent spherical diameter and zeta potential of NCC were 778 nm and -39.8 mV, respectively.
3. The sample widths of 331 µm for raw material, 5.4 µm for bleached fiber, and 26.7 nm for NFC were found. In addition, NCC was found to be 44.6 nm long and 3.7 nm width.
4. XRD analysis revealed that nanocellulose production processes increased the crystallinity index of hemp raw material. In addition, the crystallinity indexes of raw material, bleached fiber, NFC, and NCC were determined as 66.8%, 84.5%, 85.6%, and 93.7%, respectively.
5. Thermal investigations indicated that the primary thermal decompositions of hemp occurred at around 250 °C to 370 °C in raw material, 240 °C to 350 °C in bleached fiber, 220 °C to 340 °C in NFC, and 170 °C to 550 °C in NCC. Besides, it was shown that 16% of residual components were released from the raw material and bleached fiber, 25% from NFC, and 28% from NCC following thermal breakdown.
6. Chemical linkages including C–H, O–H, C–O, C–O–C, *etc*. that comprise raw material, bleached fiber, NFC, and NCC were also determined. The FTIR spectra demonstrated significant changes in the chemical structure of the samples following the applied treatments, including the removal of characteristic bonds associated with non-cellulosic

constituents. The broad O–H stretching band observed between 3400 and 3100 cm^{-1} in all samples, together with the C–H stretching vibration detected at 2981 cm^{-1}, confirms the carbohydrate-based nature of the materials. In contrast, the absorption band observed at 1748 cm^{-1} in the raw material sample is attributed to the presence of pectin, hemicellulose, and lignin. The disappearance of this band in the bleached fiber, NFC, and NCC samples indicates that the bleaching, high pressure homogenization, and acid hydrolysis treatments were effective. This finding further confirms the successful removal of hemicellulose and lignin during the processing stages.

ACKNOWLEDGMENTS

The author gratefully acknowledges the financial support provided by the Kastamonu University Scientific Research Projects Coordination Unit (Kastamonu Üniversitesi Bilimsel Araştırma Projeleri Koordinasyon Birimi, Project Number: KÜ-İHT/2024-04). The author also sincerely thanks the Hemp Research Institute of Ondokuz Mayıs University (Samsun, Türkiye); the technicians of the Kastamonu University Central Research Laboratory (Kastamonu, Türkiye); the Polymer Research Laboratory as well as the Center Research Laboratory Application and Research Center of Eskişehir Osmangazi University (Eskişehir, Türkiye) for their valuable technical assistance and support throughout this study.

REFERENCES CITED

Acar, M., and Dönmez, A. (2016). "Kenevire Farklı Bir Bakış." *2. Ulusal Biyoyakıtlar Sempozyumu Bildiriler Kitabı*, 27-30 Eylül, Samsun, Türkiye, 265-270.

Akgül, M., and Tozluoglu. A. (2009). "A comparison of soda and soda-AQ pulps from cotton stalks," *Afr. J. Biotechnol.* 8(22), 6127-6133. https://doi.org/10.5897/AJB09.301

Akinjokun A. I., Petrik, L. F., Ogunfowokan, A. O., Ajao, J., and Ojumu, T. V. (2021). "Isolation and characterization of nanocrystalline cellulose from cocoa pod husk (CPH) biomass wastes," *Heliyon* 7, 1-7. https://doi.org/10.1016/j.heliyon.2021.e06680

Alvarado, M. C., Ignacio, M. C. C. D., Acabal, M. C. G., Lapuz, A. R. P., and Yaptenco, K. F. (2024). "Review on nanocellulose production from agricultural residue through response surface methodology and its applications," *Nano Trends* 8, article 100054. https://doi.org/10.1016/j.nwnano.2024.100054

Al-Zu'bi, M., and Fan, M. (2025). "Nanocellulose technologies: Production, functionalization, and applications in medicine and pharmaceuticals – A review," *J. Biomed. Mater. Res. B Appl. Biomater.* 113, 1-16. https://doi.org/10.1002/jbm.b.35585

Amara, C., Razzak, A., Khiari, R., Dufresne, A., and Khwaldia, K. (2025). "Sustainable production of cellulose nanofibers and nanopaper sheets from olive pomace waste through mechanical defibrillation," *Biomass Conversion and Biorefinery* 15, 16619-16631. https://doi.org/10.1007/s13399-024-06296-5

Ang, S., Haritos, V., and Batchelor, W. (2019). "Effect of refining and homogenization on nanocellulose fiber development, sheet strength and energy consumption," *Cellulose* 26, 4767-4786. https://doi.org/10.1007/s10570-019-02400-5

Ateş, S., Deniz, İ., Kırcı, H., Atik, C., and Güney, K. (2011). *Türkiye'de yetişen bazı yıllık bitki artıklarının aynı tesis içerisinde değerlendirilerek kâğıt hamuru elde edilmesi ve enzimle ağartılması üzerine araştırmalar [Research on the Production of Pulp from and Enzymatic Bleaching of Residues from Certain Annual Plants Grown in Turkey, Processed Within the Same Facility]*, TÜBİTAK Projesi, No:108 O 594.

Barybina, L. O., Tkachenko, T. V., Haidai, O. O., Sokol, V. S., Korinenko, B. V., Kamenskyh, D. S., Sheludko, Y. V., Povazhny, V. A., Bohatyrenko, V. A., Ruban, S. V., Yevdokymenko, V. O. (2024). "Structural and morphological features of microcrystalline cellulose from industrial hemp hurd," *CPTS* 15(4), 524-533. https://doi.org/10.15407/hftp

Beltramino, F., Roncero, M. B., Torres, A. L., Vidal, T., and Valls, C. (2016). "Optimization of sulfuric acid hydrolysis conditions for preparation of nanocrystalline cellulose from enzymatically pretreated fibers," *Cellulose* 23, 1777-1789. https://doi.org/10.1007/s10570-016-0897-y

Beluns, S., Gaidukovs, S., Platnieks, O., Gaidukova, G., Mierina, I., Grase, L., Starkova, O., Brazdausks, P., and Thakur, V. K. (2021). "From wood and hemp biomass wastes to sustainable nanocellulose foams," *Ind Crops Prod* 170, article 113780. https://doi.org/10.1016/j.indcrop.2021.113780

Durmaz, E., and Ates, S. (2021). "Comparison of properties of cellulose nanomaterials obtained from sunflower stalks," *Cellul. Chem. Technol.* 55(7-8), 755-770. https://doi.org/10.35812/CelluloseChemTechnol.2021.55.63

Durmaz, E., and Ates, S. (2023a). "Characterization of surfaces coated with different nanocellulose-based suspensions," *Int. J. Surf. Sci. Eng*. 17(2), 141-164. https://doi.org/10.1504/IJSURFSE.2023.130169

Durmaz, E., and Ates, S. (2023b). "Effect of the nanocellulose type and matrix material on the nanocomposite film production," *Cellul. Chem. Technol*. 57(5-6), 625-635. https://doi.org/10.35812/CelluloseChemTechnol.2023.57.57

Durmaz, E., Ates, S., and Atik, C. (2025). "The effect of nanocellulose to coated paper and recycled paper," *Nord. Pulp Pap. Res. J.* 40(1), 133-147. https://doi.org/10.1515/npprj-2024-0056

Espinosa, E., Rincón, E., Morcillo-Martín, R., Rabasco-Vílchez, L., and Rodríguez, A. (2022). "Orange peel waste biorefinery in multi-component cascade approach: Polyphenolic compounds and nanocellulose for food packaging," *Ind Crop Prod* 187, 1-13. https://doi.org/10.1016/j.indcrop.2022.115413

Ganesan, A., and Rengarajan, J. (2024). "Investigating a hybrid approach for harvesting nanofibrillated cellulose from agricultural byproducts: Sugarcane bagasse and pineapple crown leaves," *Iran Polym. J.* 33, 1157-1170. https://doi.org/10.1007/s13726-024-01316-7

Gümüşkaya, E. (2002). *Chemical and Crystalline Structure Properties of Hemp (Cannabis sativa* L.*) Bast Fibres Pulp Obtained with Alkaline and Acidic Processes*, PhD Thesis, Karadeniz Technical University, Institute of Science, Trabzon.

Heacock, J. A., Sun, Y., and Li, Y. V. (2024). "Mechanical and morphological properties of cellulose nanocrystals extracted from industrial hemp agro-waste," *Cellulose* 31, 10861-10877. https://doi.org/10.1007/s10570-024-06255-3

Jamaluddin, N. A. N., Jasmani, L., Pisar, M. M., Adnan, S., Rusli, R., and Zakaria, S. (2024). "Hydrophobization of nanofibrillated cellulose from *Macaranga gigantea* for binding of curcumin," *Carbohydr Polym* 342, article 122405. https://doi.org/10.1016/j.carbpol.2024.122405

Jankowska, I., Bielejewski, M., Ławniczak, P., Pankiewicz, R., Brus, J., and Tritt-Goc, J. (2025). "Cellulose nanofibers vs. cellulose nanocrystals: a comparative study on their influence on the properties of imidazole-doped proton-conducting nanocomposites," *Cellulose* 32, 4763-4779. https://doi.org/10.1007/s10570-025-06559-y

Jasmani, L., Jamaluddin, N. A. N., Rusli, R., Adnan, S., and Zakaria, S. (2022). "Different preparation method of nanocellulose from *macaranga gigantea* and its preliminary study on packaging film potential," *Polymers* 14(21), article 4591. https://doi.org/10.3390/polym14214591

Jiang, W., and Gu, J. (2020). "Nanocrystalline cellulose isolated from different renewable sources to fabricate natural rubber composites with outstanding mechanical properties," *Cellulose* 27, 5801-5813. https://doi.org/10.1007/s10570-020-03209-3

Kian, L. K., Jawaid, M., Ariffin, H., and Karim, Z. (2018). "Isolation and characterization of nanocrystalline cellulose from roselle-derived microcrystalline cellulose," *Int. J. Biol. Macromol.* 114, 54-63. https://doi.org/10.1016/j.ijbiomac.2018.03.065

Krishnadev, P., Subramanian, K. S., Janavi, G. J., Ganapathy, S., and Lakshmanan, A. (2020). "Synthesis and characterization of nano-fibrillated cellulose derived from green *Agave americana* L. fiber," *BioResources* 15(2), 2442-2458. https://doi.org/10.15376/biores.15.2.2442-2458

Lawson, L., Degenstein, L. M., Bates, B., Chute, W., King, D., and Dolez, P. I. (2022). "Cellulose textiles from hemp biomass: Opportunities and challenges," *Sustainability* 14(22), article 15337. https://doi.org/10.3390/su142215337

Lee, B. M., Jeun, J. P., Kang, P. H., Choi, J. H., and Hong, S. K. (2017). "Isolation and characterization of nanocrystalline cellulose from different precursor materials," *Fiber Polym* 18(2), 272-277. https://doi.org/10.1007/s12221-017-6548-6

Li, X., Wang, S., Du, G., Wu, Z., and Meng, Y. (2013). "Variation in physical and mechanical properties of hemp stalk fibers along height of stem," *Ind Crop Prod* 42, 344-348. https://doi.org/10.1016/j.indcrop.2012.05.043

Lu, P., and Hsieh, Y. L. (2012). "Preparation and characterization of cellulose nanocrystals from rice straw," *Carbohydr Polym* 87, 564-573. https://doi.org/10.1016/j.carbpol.2011.08.022

Mahesh, S., Kumar, P., and Ansari, S. A. (2015). "A rapid and economical method for the maceration of wood fibers in *Boswellia serrata* Roxb.," *Trop Plant Res* 2(2), 108-111.

Manaia, J. P., Manaia, A. T., and Rodriges, L. (2019). "Industrial hemp fibers: An overview," *Fibers* 7(12), 106. https://doi.org/10.3390/fib7120106

Manian, A. P., Cordin, M., and Pham, T. (2021). "Extraction of cellulose fibers from flax and hemp: a review," *Cellulose* 28, 8275-8294. https://doi.org/10.1007/s10570-021-04051-x

Mo, Y., Huang, X., Yue, M., Hu, L., and Hu, C. (2024). "Preparation of nanocellulose and application of nanocellulose polyurethane composites," *RSC Adv* 14, 18247-18257. https://doi.org/10.1039/D4RA01412J

Nagarajan, K. J., Ramanujam, N. R., Sanjay, M. R., Siengchin, S., Rajan, B. S., Basha, K. S., Madhu, P., and Raghav, G. R. (2021). "A comprehensive review on cellulose nanocrystals and cellulose nanofibers: Pretreatment, preparation, and characterization," *Polymer Composites* 42, 1588-1630. https://doi.org/10.1002/pc.25929

Norfarhana, A. S., Ilyas, R. A., Nordin, A. H., Ismail, Y. M. N. S., Ngadi, N., and Othman, M. H. D. (2025). "Development and performance of sugar palm nano-fibrillated cellulose reinforced rubber membranes for efficient palm oil mill effluent

treatment," *J. Water Process Eng.* 72, 1-13. https://doi.org/10.1016/j.jwpe.2025.107527

Padhi, S., Singh, A., and Routray, W. (2023). "Nanocellulose from agro-waste: A comprehensive review of extraction methods and applications," *Rev. Environ. Sci. Biotechnol.* 22, 1-27. https://doi.org/10.1007/s11157-023-09643-6

Ratnakumar, A., Samarasekara, A. M. P. B., Amarasinghe, D. A. S., and Karunanayake, L. (2021). "Individualization of nanofibrillated cellulose from Sri Lankan rice straw: Structural characteristics and thermal properties," in: *Moratuwa Engineering Research Conference (MERCon)*, pp. 37-42.

Reddy, N., and Yang, Y. (2005). "Structure and properties of high quality natural cellulose fibers from cornstalks," *Polymer* 46, 5494-5500. https://doi.org/10.1016/j.polymer.2005.04.073

Singh, M., Pahal, V., and Ahuja, D. (2020). "Isolation and characterization of microfibrillated cellulose and nanofibrillated cellulose with "biomechanical hotspots"," *Carbohydr Polym* 234, article 115827. https://doi.org/10.1016/j.carbpol.2020.115827

Stanislas, T. T., Tendo, J. F., Ojo, E. B., Ngasoh, O. F., Onwualu, P. A., Njeugna, E., and Junior, H. S. (2022). "Production and characterization of pulp and nanofibrillated cellulose from selected tropical plants," *J. Nat. Fibers* 19(5), 1592-1608. https://doi.org/10.1080/15440478.2020.1787915

Sukhikh, S., Babich, O., Ivanova, S., Kriger, O., Prosekov, A., Noskova, S., Ulrikh, E., Budenkova, E., and Kalashnikova, O. (2024). "Production of nanocellulose from miscanthus biomass," *Curr. Res. Green Sustain Chem.* 8, article 100412. https://doi.org/10.1016/j.crgsc.2024.100412

Tank, T., Göksel, E., Cengiz, M., and Gürboy, B. (1990). "Hızlı gelişen bazı iğne yapraklı ağaç türlerinin lif ve kağıt teknolojisi yönünden incelenmesi [Investigation of certain fast-growing coniferous tree species from the perspective of fiber and paper technology]," *İstanbul Üniversitesi Orman Fakültesi Dergisi A*, 40(1), 40-54.

TAPPI T222 om-02. (2002). "Acid-insoluble lignin in wood and pulp," TAPPI Press, Atlanta, GA.

TAPPI T204 cm-97. (1997). "Solvent extractives of wood and pulp," TAPPI Press, Atlanta, GA.

TAPPI T211 om-02. (2002). "Ash in wood, pulp, paper and paperboard: combustion at 525°C," TAPPI Press, Atlanta, GA.

TAPPI T207 cm-99. (1999). "Water solubility of wood and pulp," TAPPI Press, Atlanta, GA.

TAPPI T203 cm-99. (1999). "Alpha-, beta- and gamma-cellulose in pulp," TAPPI Press, Atlanta, GA.

TAPPI T212 om-12. (2012). "One percent sodium hydroxide solubility of wood and pulp," TAPPI Press, Atlanta, GA.

TAPPI T264 om-07. (2007). "Preparation of wood for chemical analysis," TAPPI Press, Atlanta, GA.

Tiwari, A., and Sanjog, J. (2025). "Morphological, structural, and thermal properties of cellulose nanocrystals extracted from Indian water chestnut shells (agricultural waste)," *Next Mater* 8, article 100653. https://doi.org/10.1016/j.nxmate.2025.100653

Tyagi, P., Gutierrez, J. N., Nathani, V., Lucia, L. A., Rojas, O. J., Hubbe M. A., and Pal, L. (2021). "Hydrothermal and mechanically generated hemp hurd nanofibers for

sustainable barrier coatings/films," *Ind. Crop. Prod.* 168, article 113582. https://doi.org/10.1016/j.indcrop.2021.113582

Vivek, V. (2019). "The usages of every part of hemp plant," (https://hempfoundation.net/the-usages-of-every-part-of-hemp-plant/), accessed 14 December 2019.

Vu, A. N., Nguyen, L. H., Tran, H. C. V., Yoshimura, K., Tran, T. D., Le, H. V., and Nguyen, N. U. T. (2024). "Cellulose nanocrystals extracted from rice husk using the formic/peroxyformic acid process: isolation and structural characterization," *RSC Adv.* 14, 2048-2060. https://doi.org/10.1039/D3RA06724F

Wang, Y., Wang, Z., Lin, Y., Qin, Y., He, R., Wang, M., Sun, Q., and Peng, Y. (2024). "Nanocellulose from agro-industrial wastes: A review on sources, production, applications, and current challenges," *Food Res Int* 192, article 114741. https://doi.org/10.1016/j.foodres.2024.114741

Wise, L. E., Murphy, M., and D'Adieco, A. A. (1946). "Chlorite holocellulose, its fractionation and bearing on summative wood analysis and studies on the hemicelluloses," *Paper Trade* 122(2), 35-43. CABI Record Number: 19460600433

Wossine, S. E., Thothadri, G., Tufa, H. B., Tucho, W. M., Murtaza, A., Edacherian, A., and Ahmed, G. M. S. (2024). "Isolation and characterization of spherical cellulose nanocrystals extracted from the higher cellulose yield of the Jenfokie plant: Morphological, structural, and thermal properties," *Polymers* 16(12), article 1629. https://doi.org/10.3390/polym16121629

Xu, J., Krietemeyer, E. F., Boddu, V. M., Liu, S. X., and Liu, W. C. (2018). "Production and characterization of cellulose nanofibril (CNF) from agricultural waste corn stover," *Carbohydr Polym* 192, 202-207. https://doi.org/10.1016/j.carbpol.2018.03.017

Zhang, Z., Liu, X., Wang, H., He, H., and Bai, R. (2020). "Preparation and characterization of *Enteromorpha prolifera* nanocellulose/polyvinyl alcohol composite films," *Polym Compos* 42(4), 1712-1726. https://doi.org/10.1002/pc.25926

Zhong, J., Xie, H., Wang, Y., Xiong, H., and Zhao, Q. (2024). "Nanofibrillated cellulose derived from rice bran, wheat bran, okara as novel dietary fibers: Structural, physicochemical, and functional properties," *Int. J. Biol. Macromol.* 273, article 132902. https://doi.org/10.1016/j.ijbiomac.2024.132902

Article submitted: May 12, 2026; Peer review completed: June 13, 2026; Revised version received: June 22, 2026; Accepted: June 29, 2026; Published: July 9, 2026.
DOI: 10.15376/biores.21.3.7893-7911